

CORROSION EFFECT ON STRESS CONCENTRATION FACTOR IN TUBULAR T-JOINTS UNDER AXIAL LOADING

Vu Dan Chinh^{a,*}, Do Thanh Long^a

^a*Faculty of Coastal and Offshore Engineering, Ha Noi University of Civil Engineering,
55 Giai Phong road, Hai Ba Trung district, Hanoi, Vietnam*

Article history:

Received 11/01/2023, Revised 11/02/2023, Accepted 17/03/2023

Abstract

A stress concentration factor (SCF) is used to determine concentrated stress at hotspots for fatigue evaluation of steel fixed offshore platforms. The varying SCF significantly affects the fatigue damage of the hotspot according to the exponential function. Current standards have proposed empirical formulas to determine the SCF at the hotspots of the tubular joints, but it depends on the geometry and some specific limitations. When a tubular joint is corroded, its geometry will be changed, making these limitations unsuitable, especially for the case of non-uniform corrosion. Therefore the formulas are no longer suitable to apply in these cases. This paper uses ABAQUS-based numerical simulation to analyze concentrated stress at saddle and crown points on the chord of non-uniform corroded tubular T-joints under axial loading in some different scenarios. The research indicates that thickness and dimension of corroded zone around the joint intersection substantially influence stress concentration factor and fatigue damage at the mentioned hotspots.

Keywords: SCF; concentrated stress; tubular T-joints; non-uniform corrosion; numerical simulation.

[https://doi.org/10.31814/stce.huce2023-17\(3\)-12](https://doi.org/10.31814/stce.huce2023-17(3)-12) © 2023 Hanoi University of Civil Engineering (HUCE)

1. Introduction

The most dangerous fatigue damage in fatigue analysis usually occurs at the stress concentration points. These points are called hotspots. Generally, the hotspot stress can be determined directly through experiments or numerical computations.

In the steel fixed offshore platform, the hotspots are mainly located at the intersection of tubular joints. Consequently, the concentrated stress is determined by a rate with nominal values through the SCF. These coefficients are estimated through given empirical formulae that depend on the joint shape and geometrical dimensions, such as the formulae of Efthymiou, Kuang, Wordsworth/Smedley [1–3]. These formulae have also been recommended in current design standards such as API [4], DnV [5], and Lloyd's Register [6], ... However, the above formulae have some limitations, summarised as: Cross-sections are circles; Brace-to-chord width ratio, the ratio between diameter, thickness, and length of the chord, the gap between braces, etc., must be in the valid application.

In the fatigue calculation of the above standards, corrosion is mentioned through a loss thickness that is uniformly applied on the entire tube and tubular joints. This value is usually calculated as half of the allowable corrosion thickness over the lifetime of the structure. Therefore, the SCF at hot spots is always assumed to be constant when assessing the loss and fatigue life of the structure. However, when the tubular joints are corroded non-uniformly as shown in Fig. 1, two different problems can happen as below:

- Corroded joint geometry is outside the application range of standard-based formulae;
- The SCF varies over time corresponding to the development of both corroded thickness and area.

*Corresponding author. E-mail address: chinhvd@huce.edu.vn (Chinh, V. D.)

Since the relationship between fatigue damage and stress concentration is proportional to the exponential function [4, 7], a slight variation in the SCF also causes significant changes in fatigue damage and structural life. Therefore, the influence of uneven corrosion on the SCF of the tubular joints needs to be studied in more detail. There are relevant literature reviews on the SCF in corroded offshore structures published recently [8–11]. However, the above studies focused on measuring and determining the SCF at new hotspots occurring in deep holes caused by local corrosion and located outside the weld area at the joint intersection.

The paper mainly focuses on the thickness-and-dimension influences in the corroded area on the variation of SCF at the saddle and crown points on the tubular chord under axial loading to clarify the above differences in non-uniform corrosion over time. In tubular joints with complicated shapes and geometries, the best method is to measure the SCF through experimental laboratories. However, numerical analysis is becoming popular and reliable with the development of calculation methods and computations. Relevant studies can be mentioned in research [12–15]. Herein, the Abaqus-based numerical method is used to conduct calculations. More detail will be presented in the following sections.

2. Methodology of SCF for tubular T-joint under axial loading

2.1. Calculations based on experimental equations

Considering a tubular T-joint with fixed ends, subjected to longitudinal force P (Fig. 2). Let D, T and d, t be the outer diameter and thickness of the chord and brace, respectively. A basic formula determines the nominal stress on the brace, mentioned in Eq. (1):

$$\sigma_n = \frac{P}{A} \quad (1)$$

where A is the cross-sectional area of the brace, $A = \frac{\pi}{4}(d^2 - (d - 2t)^2)$.

Concentrated stress at the saddle point σ_{SC} and the crown point σ_{CC} are determined as the formulae (2)

$$\sigma_{SC} = SCF_{SC} \cdot \sigma_n; \quad \sigma_{CC} = SCF_{CC} \cdot \sigma_n \quad (2)$$

where SCF_{SC} and SCF_{CC} are SCFs at the saddle and crown points, respectively.

The SCF formulae at the hotspots on the chord with fixed ends based on API and Lloyd's Register standards depend on the geometric characteristics of joints, summarized in Table 1.

Note that the above formulae are applied for the brace-and-chord joints with circle sections. Furthermore, the condition given in Table 2 should be satisfied.



Figure 1. A corroded tubular joint on Jacket MSP 6 at the White Tiger field

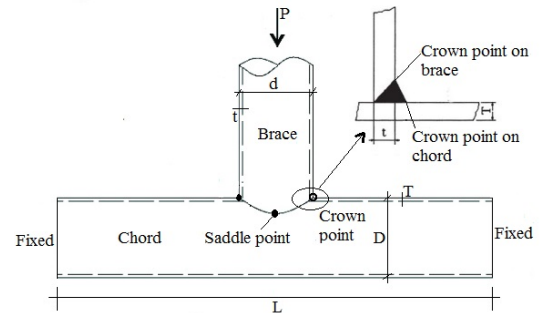


Figure 2. Tubular T-joint and hotspots

Table 1. SCF formulae in API and Lloyd's Register

Hot spot	SCF	
	API	Lloyd's Register
Saddle point	$SCF_{SC} = \gamma\tau^{1.1}(1.11 - 3(\beta - 0.52)^2)$ (3)	$SCF_{SC} = \tau\gamma^{1.2}\beta(2.12 - 2\beta)$ (4)
Peak point	$SCF_{CC} = \gamma^{0.2}\tau(2.65 + 5(\beta - 0.65)^2) + \tau\beta(0.25\alpha - 3)$ (5)	$SCF_{CC} = \gamma^{0.2}\tau(3.5 - 2.4\beta) + \left(\frac{0.5\tau(\beta - \frac{\tau}{2\gamma})(\frac{\alpha}{2} - \beta)}{1 - \frac{3}{2\gamma}}\right)\left(1.05 + \frac{4.5\tau^{1.5}(1.2 - \beta)}{\gamma}\right)$ (6)

where $\alpha = \frac{2L}{D}$; $\beta = \frac{d}{D}$; $\gamma = \frac{D}{2T}$; $\tau = \frac{t}{T}$.

Table 2. Valid application of formulae in API và Lloyd's Register

Parameters	α	β	γ	τ
API	4 - 40	0.2 - 1	12 - 32	0.2 - 1
Lloyd's Register	≥ 4	0.13 - 1	12 - 35	0.25 - 1

2.2. Numerical model

Tubular joints are simulated by the ABAQUS [16, 17]. Some essential calculations are briefly summarized as follows:

- Tubular joints are modeled based on geometric data with given shapes and dimensions. In the formulae above, the effect of welding is ignored. Tubular joints are simulated by shell elements to reduce computational time and make a rapid change in thickness.
- Creating two reference points RP2 and RP3 at both ends of the chord for fixed supports and one reference point RP1 at the top of the brace for the axial load as in Fig. 3.
- Using the meshing method with 4-node quadrilateral finite elements (S4R). The dimension of elements is chosen to ensure the convergence of stress at the intersection between the brace and the chord (Fig. 4). This paper does not aim to study the influence of mesh geometry on the strength of the pipe. However, some cases will be selected for evaluation in models. The calculation results show that with the element size of 2 cm, the value of stress has converged.

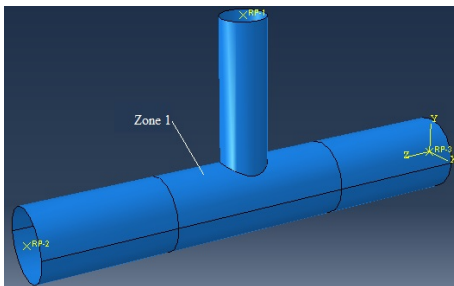


Figure 3. Numerical model of tubular T-joints in Abaqus

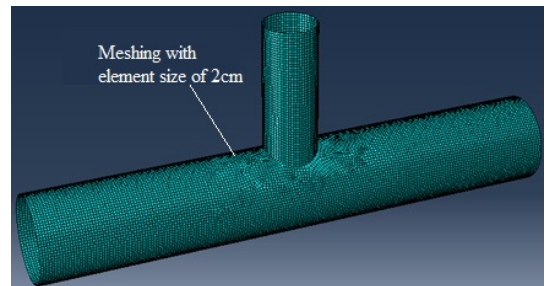


Figure 4. Meshing grid in Abaqus

- For corroded tube joints, this paper focuses on corroded defects occurring in Zone 1, which affects significant concentrated stress, with the length of L_{z1} and height of $0.5D - h$ (Figs. 3 and 5). According to a study [18, 19], the segment of the chord affected by force on the brace is $L_e = 2 \times 6\sqrt{DT}$. Therefore, Zone 1 is limited to a range $L_{z1} \leq L_e$. The height of Zone 1 is considered within the upper half of the main pipe.

- Due to corrosion occurring from outside, it is necessary to modify the coordinate of meshing points on the corrosion part of zone 1 (Fig. 6).

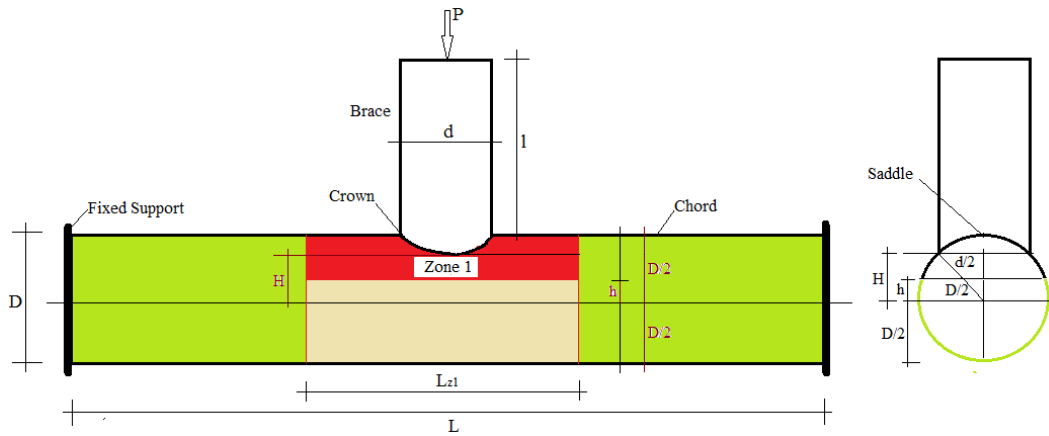


Figure 5. Model of corroded tubular T-joint

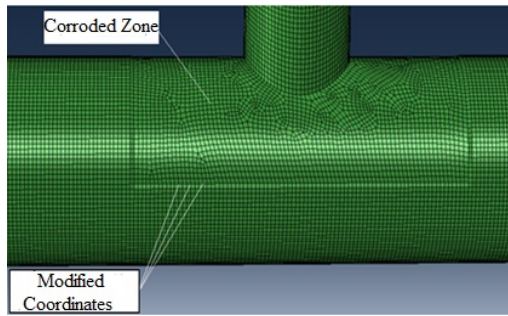


Figure 6. Model of corrosion zone on tubular joints

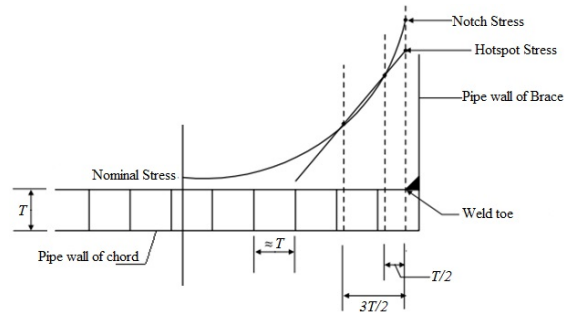


Figure 7. Definition of the hotspot stress of tubular joints

For any point on the chord with a corrosion thickness of ΔT , the new coordinate components x_c, y_c are satisfied the equations:

$$x_c = \frac{\frac{D}{2} - \Delta T}{\frac{D}{2}} x; \quad y_c = \frac{\frac{D}{2} - \Delta T}{\frac{D}{2}} y \quad (7)$$

where x, y are the old coordinates of that point pre-corrosion.

- The value of axial force at the top of the brace is selected to ensure that the tubular joint works in a linear elastic phase.

2.3. Determination of SCFs based on the numerical simulation

In the ABS standard [20], based on numerical analysis results, the hotspot stress will be determined through linear extrapolation from the stress values at distances of $T/2$ and $3T/2$ from the weld toe (Fig. 7). The SCFs at the saddle and crown points are determined by the ratio of the hotspot stress over the nominal stress based on the formula (1).

3. Results and Discussions

3.1. Validation in the numerical model of intact tubular T-joints

Intact tubular T-joints are considered as mentioned in Table 3. The SCFs at hotspots on chords are performed based on API, Lloyd's register standards, and the ABAQUS program. The analysis

results are summarized in Tables 4 and 5. The configuration of concentrated stresses on the joints is presented in Fig. 8.

Table 3. Data of intact tubular T-joints

Case id.	$D \times T$ (mm)	$d \times t$ (mm)	L (m)	l (m)	Constraint
TH 1	813×25	508×16	5	2	Fixed
TH 2	813×20	508×16	5	2	Fixed
TH 3	813×16	508×16	5	2	Fixed
TH 4	1020×30	610×16	6.5	2	Fixed
TH 5	1020×25	610×16	6.5	2	Fixed
TH 6	1020×20	610×16	6.5	2	Fixed
TH 7	1270×30	813×19	8	2	Fixed
TH 8	1270×25	813×19	8	2	Fixed
TH 9	1270×20	813×19	8	2	Fixed

Table 4. SCF at hotspots on chords based on API and Lloyd's register

Case id.	API		Lloyd's Register	
	SCF of saddle	SCF of crown	SCF of saddle	SCF of crown
TH 1	10.7	3.0	9.9	3.3
TH 2	17.1	3.9	16.2	4.2
TH 3	27.3	5.1	26.4	5.5
TH 4	9.3	2.6	8.8	2.8
TH 5	13.6	3.2	13.2	3.5
TH 6	21.8	4.2	21.5	4.5
TH 7	13.7	3.2	13.3	3.4
TH 8	20.0	3.9	19.8	4.2
TH 9	32.0	5.1	32.4	5.4

Table 5. SCF at hotspots on chords based on ABAQUS-derived numerical analysis

Case id.	Axial load (MN)	Nominal stress (MPa)	Stress at saddle points (MPa)	SCF at saddle	Stress at crown points (MPa)	SCF at crown
TH 1	0.3	12.21	123.2	10.1	35.3	2.9
TH 2	0.3	12.21	196.0	16.1	47.6	3.9
TH 3	0.3	12.21	305.2	25	62.2	5.1
TH 4	0.5	16.90	152.1	9.0	40.6	2.4
TH 5	0.5	16.90	224.8	13.3	50.7	3.0
TH 6	0.5	16.90	348.1	20.6	67.6	4.0
TH 7	0.5	10.64	153.2	14.4	35.1	3.3
TH 8	0.5	10.64	220.3	20.7	46.8	4.4
TH 9	0.5	10.64	341.5	32.1	58.5	5.5

Figs. 9 and 10 present the comparison of SCF at the intact tubular T-joints based on the standards and numerical analysis. Clearly, the SCF results of saddle points in the three methods are comparable.

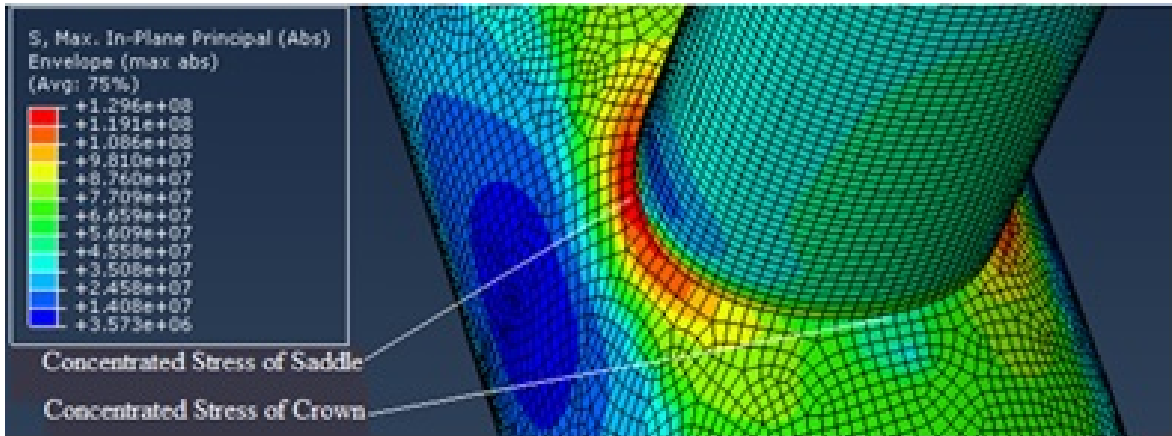


Figure 8. Concentrated stress distribution of a typical tubular T-joint

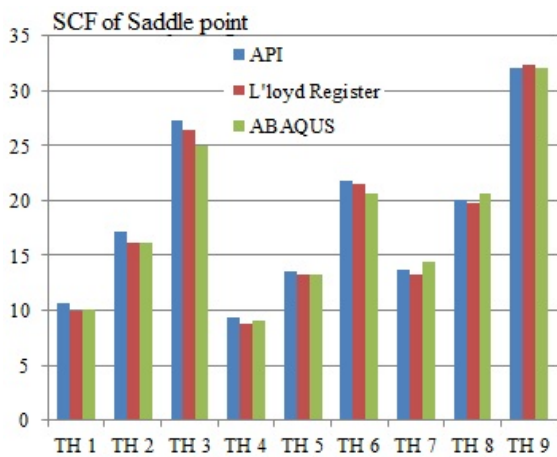


Figure 9. SCF of saddle points

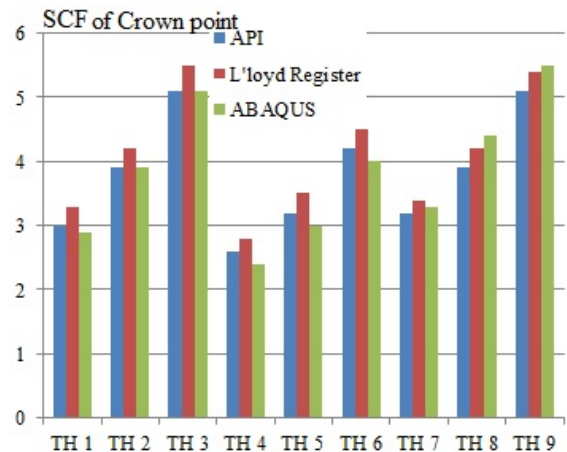


Figure 10. SCF of crown points

The maximum error is approximately 6%. For crown points, the results are relatively similar. The results based on Lloyd's Register are the largest and have the biggest difference, approximately 17%, from the other two methods. However, the SCF of crown points is quite small, so the difference doesn't cause significant effects on fatigue damage.

3.2. Effect of corrosion on SCF

Corroded thickness and area of zone 1 (Fig. 5) have a certain influence on the SCF at hotspots on the chord. The degree of change existing in the factors is investigated by numerical analysis of tubular T-joints in various corrosion tests. The input data is listed in Table 6. Results are presented in Fig. 11 to Fig. 16.

3.3. Influence of the SCF variation on fatigue damage at hotspot

The predicted number of cycles to fatigue failure N of a hotspot is determined based on the exponentiation function of hotspot stress range S as Eq. (8):

$$N = aS^{-m} \quad (8)$$

whereas a and m are experimental coefficients. For tubular joints, the API standard gives $m = 3 \div 5$ depending on hotspot properties and the number of cycles of loading.

Table 6. Data of corroded tubular T-joints

Case id.	$D \times T$ (mm)	$d \times t$ (mm)	L (m)	l (m)	T_{z1} (mm)	h (m)	L_{z1} (m)
TH 10	813×25	508×16	5	2	20	0	2
TH 11	813×25	508×16	5	2	20	0.2	2
TH 12	813×25	508×16	5	2	20	0.28	2
TH 13	813×25	508×16	5	2	20	0.28	0.6
TH 14	813×25	508×16	5	2	16	0	2
TH 15	813×25	508×16	5	2	16	0.2	2
TH 16	813×25	508×16	5	2	16	0.28	2
TH 17	813×25	508×16	5	2	16	0.28	0.6
TH 18	1020×30	610×16	6.5	2	25	0	2.5
TH 19	1020×30	610×16	6.5	2	25	0.3	2.5
TH 20	1020×30	610×16	6.5	2	25	0.35	2.5
TH 21	1020×30	610×16	6.5	2	25	0.35	0.8
TH 22	1020×30	610×16	6.5	2	20	0	2.5
TH 23	1020×30	610×16	6.5	2	20	0.3	2.5
TH 24	1020×30	610×16	6.5	2	20	0.35	2.5
TH 25	1020×30	610×16	6.5	2	20	0.35	0.8
TH 26	1270×30	813×19	8	2	25	0	2.5
TH 27	1270×30	813×19	8	2	25	0.35	2.5
TH 28	1270×30	813×19	8	2	25	0.43	2.5
TH 29	1270×30	813×19	8	2	25	0.43	1.0
TH 30	1270×30	813×19	8	2	20	0	2.5
TH 31	1270×30	813×19	8	2	20	0.35	2.5
TH 32	1270×30	813×19	8	2	20	0.43	2.5
TH 33	1270×30	813×19	8	2	20	0.43	1.0

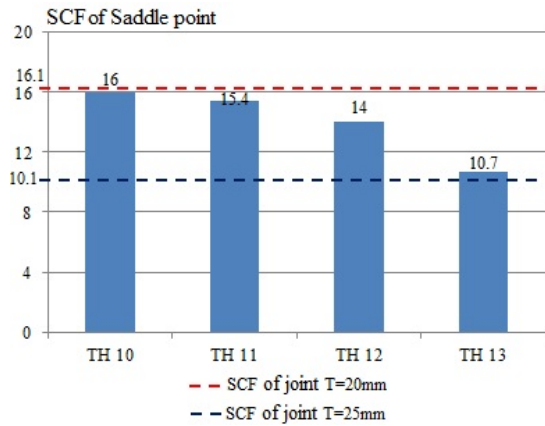
Let S_n be the nominal stress range of the hotspot ($S_n = \sigma_{n \max} - \sigma_{n \min}$), so Eq. (8) can be re-written below:

$$N = a(SCF.S_n)^{-m} \quad (9)$$

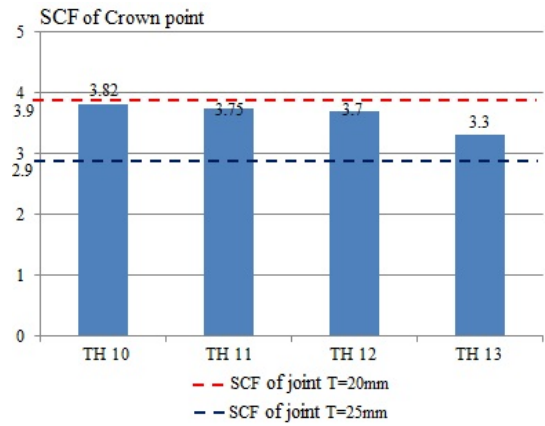
From formula (9), it is easy to see that when SCF increases by k times, the number of cycles to fatigue failure N is reduced by k^m , which means that the fatigue damage increases by k^m , and vice versa. Assuming the corrosion thickness measured every year and the pipe thickness for one year are constant. The ratio of the fatigue damages in the year corresponding to the corrosion thicknesses and the fatigue damage in the first year is calculated. The results are summarized in Table 7.

3.4. Discussions

- The results in Table 5 show that the SCF has significant changes when the pipe thickness changes, according to the inverse relationship. The maximum in the increased rate of SCF is roughly 1.6 corresponding to a reduced ratio of the chord thickness of 25%, and ≈ 2.5 for a reduced ratio of chord thickness of 36%.

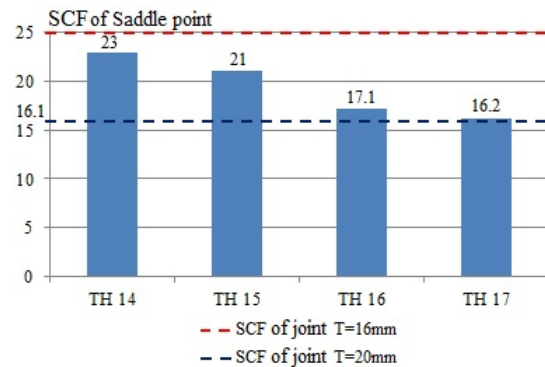


(a) SCF of Saddle point

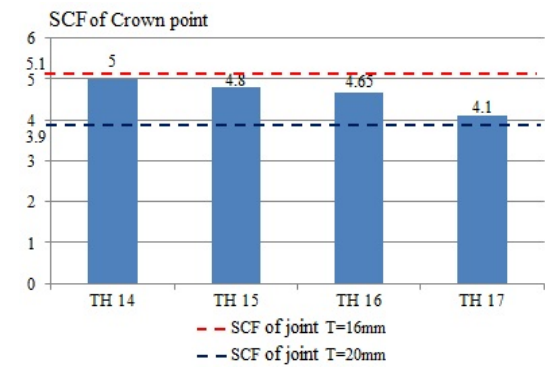


(b) SCF of Crown point

Figure 11. SCFs of saddle and crown points on a chord of corroded tubular T-joint Cases TH 10, TH 11, TH 12, TH 13

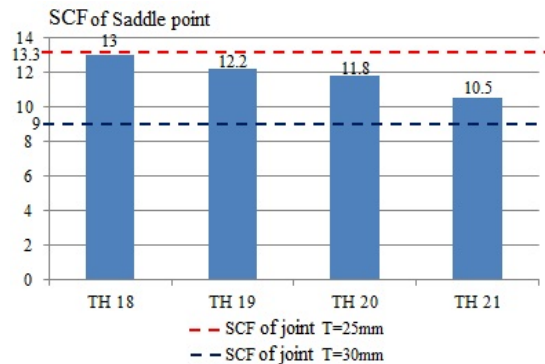


(a) SCF of Saddle point

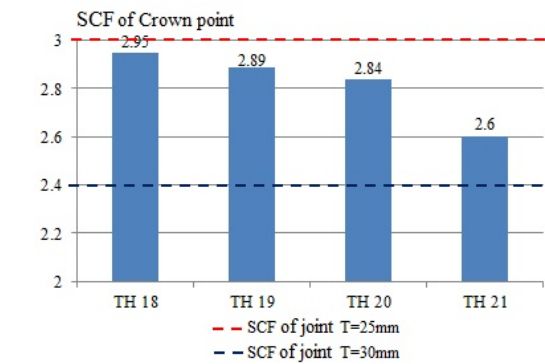


(b) SCF of Crown point

Figure 12. SCFs of saddle and crown points on a chord of corroded tubular T-joint Cases TH 14, TH 15, TH 16, TH 17

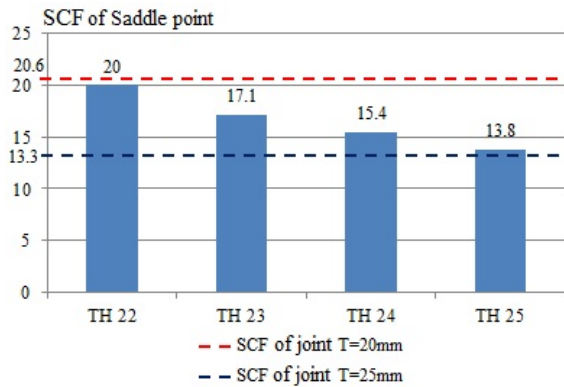


(a) SCF of Saddle point

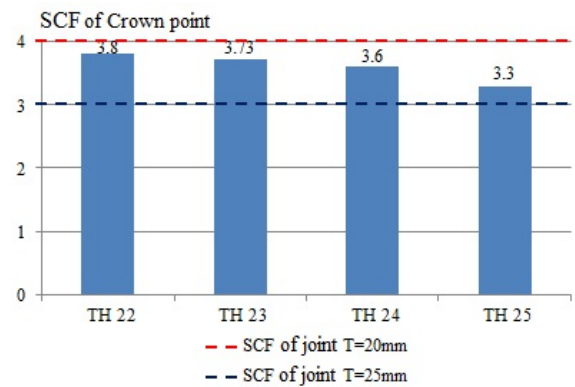


(b) SCF of Crown point

Figure 13. SCFs of saddle and crown points on a chord of corroded tubular T-joint Cases TH 18, TH 19, TH 20, TH 21

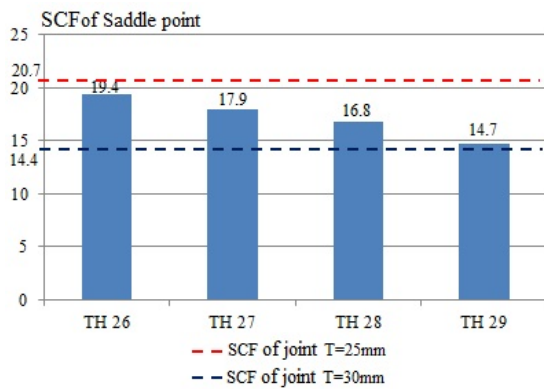


(a) SCF of Saddle point

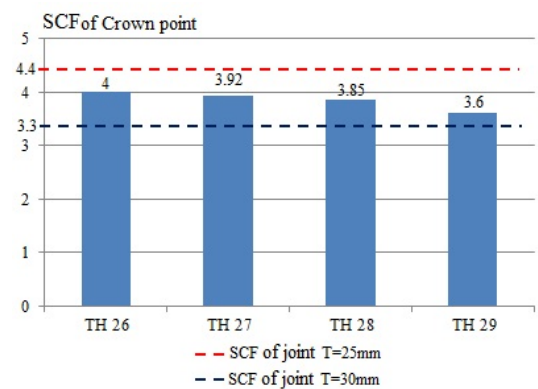


(b) SCF of Crown point

Figure 14. SCF's results of saddle and crown points on a chord of corroded tubular T-joint Cases TH 22, TH 23, TH 24, TH 25

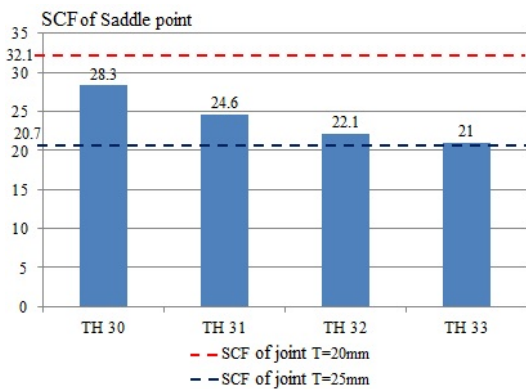


(a) SCF of Saddle point

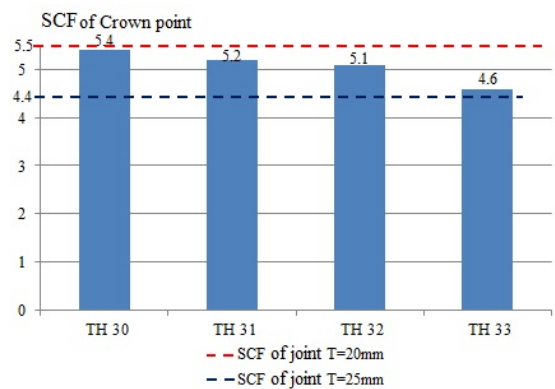


(b) SCF of Crown point

Figure 15. SCF's results of saddle and crown points on a chord of corroded tubular T-joint Cases TH 26, TH 27, TH 28, TH 29



(a) SCF of Saddle point



(b) SCF of Crown point

Figure 16. SCF's results of saddle and crown points on a chord of corroded tubular T-joint Cases TH 30, TH 31, TH 32, TH 33

Table 7. Increased rate between fatigue damage of corroded joint and intact joint corresponding to stress range S_n

Case id.	Corrosion Thickness (mm)	SCF of Saddle point of intact joint (SCF _{sn})	SCF of Saddle point of corroded joint (SCF _{sc})	ks = SCF _{sc} /SCF _{sn}	SCF of Crown point of intact joint (SCF _{cn})	SCF of Crown point of corroded joint (SCF _{cc})	kc = SCF _{cc} /SCF _{cn}	Increased rate of fatigue damage for $m = 3$	
								Saddle point	Crown point
TH10	5	10.1	16	1.58	2.9	3.82	1.32	3.98	2.29
TH11	5	10.1	15.4	1.52	2.9	3.75	1.29	3.54	2.16
TH12	5	10.1	14	1.39	2.9	3.7	1.28	2.66	2.08
TH13	5	10.1	10.7	1.06	2.9	3.3	1.14	1.19	1.47
TH14	9	10.1	23	2.28	2.9	5	1.72	11.81	5.13
TH15	9	10.1	21	2.08	2.9	4.8	1.66	8.99	4.53
TH16	9	10.1	17.1	1.69	2.9	4.65	1.60	4.85	4.12
TH17	9	10.1	16.2	1.60	2.9	4.1	1.41	4.13	2.83
TH18	5	9	13	1.44	2.4	2.95	1.23	3.01	1.86
TH19	5	9	12.2	1.36	2.4	2.89	1.20	2.49	1.75
TH20	5	9	11.8	1.31	2.4	2.84	1.18	2.25	1.66
TH21	5	9	10.5	1.17	2.4	2.6	1.08	1.59	1.27
TH22	10	9	20	2.22	2.4	3.8	1.58	10.97	3.97
TH23	10	9	17.1	1.90	2.4	3.73	1.55	6.86	3.75
TH24	10	9	15.4	1.71	2.4	3.6	1.50	5.01	3.38
TH25	10	9	13.8	1.53	2.4	3.3	1.38	3.61	2.60
TH26	5	14.4	19.4	1.35	3.3	4	1.21	2.45	1.78
TH27	5	14.4	17.9	1.24	3.3	3.92	1.19	1.92	1.68
TH28	5	14.4	16.8	1.17	3.3	3.85	1.17	1.59	1.59
TH29	5	14.4	14.7	1.02	3.3	3.6	1.09	1.06	1.30
TH30	10	14.4	28.3	1.97	3.3	5.4	1.64	7.59	4.38
TH31	10	14.4	24.6	1.71	3.3	5.2	1.58	4.99	3.91
TH32	10	14.4	22.1	1.53	3.3	5.1	1.55	3.61	3.69
TH33	10	14.4	21	1.46	3.3	4.6	1.39	3.10	2.71

- According to the results in Figs. 8 to 13, SCF is proportional to corrosion area. For a corrosion thickness, SCF can be increased ≈ 1.5 times when the corrosion area increases with the length $L_{z1} = L_e$ and the height $= 0.5D$. When the corrosion area exceeds the limits, the SCF is almost unchanged.

- The corrosion dimension affects the SCF at the saddle point more significantly than the crown point. The maximum difference of the SCF at the saddle point is roughly 7.3, whereas at the crown point is only 0.9. In which, the corroded height has more impact than its length.

- According to the results in Table 7, the maximum increased rate of SCF between non-uniform corroded tubular joint and intact tubular joint ranges from 1.02 to 2.28 times. So the ratio between fatigue damage of corroded hotspots over the intact ones ranges from 1.06 to 11.8 times. It shows that the influence of the corrosion scenario on fatigue damage is very significant and should be studied in more detail.

4. Conclusions

Conclusions can be made based on analysis of the above numerical models of tubular T-joints:

Corrosion has a large influence on the SCF at hotspots on the chord. The influential level depends on corrosion thickness and area.

Corrosion thickness is the main factor affecting the SCF, but the height and length of the corrosion area also have a significant influence. The SCF is proportional to all these parameters. However, when the corrosion area expands with a length exceeding L_e and a height exceeding $0.5D$, the SCF mainly depends on the thickness.

In order to predict precisely the fatigue loss at a non-uniform corroded joint, it is necessary to take into account the change of the SCF corresponding to the change of both the corroded thickness and area size based on periodic surveys.

The influence of the thickness, length, and height of the corrosion area on the SCF of hotspots of different types of tubular joints will be specified by the formula in the next studies. These formulas will be built and verified through numerical and physical models, to support the current standard in appropriate cases.

Acknowledgments

The research described in this paper was financially supported by the Ministry of Education and Training in Scientific Project number B2021-XDA-04.

References

- [1] Lloyd Register of Shipping (1997). *Stress concentration factors for simple tubular joints*. OnePetro, Health and Safety Executive - Offshore Technology Report. ISBN 0-7176-1418-2.
- [2] Atteya, M., Mikkelsen, O., Wintle, J., Ersdal, G. (2021). [Experimental and Numerical Study of the Elastic SCF of Tubular Joints](#). *Materials*, 14(15):4220.
- [3] Saini, D. S., Karmakar, D., Ray-Chaudhuri, S. (2016). [A review of stress concentration factors in tubular and non-tubular joints for design of offshore installations](#). *Journal of Ocean Engineering and Science*, 1 (3):186–202.
- [4] API (2007). *Recommended Practice for Planning, Designing and Constructing Fixed Offshore Platforms*. American Petroleum Institute Publication RP-2A, Dallas, Texas, USA.
- [5] DnV (2010). *Fatigue Design of Offshore Steel Structures*. DnV RP C203.
- [6] Lloyd Register (2022). *Rules for the Classification of Offshore Units*. Lloyd's Register Group Limited.
- [7] Chinh, V. Đ., Cường, Đ. Q. (2014). An estimation of static stress effects on fatigue life of fixed steel offshore structures in Vietnam sea conditions. *Journal of Science and Technology in Civil Engineering (STCE) - HUCE*, 21.
- [8] Shojai, S., Schaumann, P., Braun, M., Ehlers, S. (2022). [Influence of pitting corrosion on the fatigue strength of offshore steel structures based on 3D surface scans](#). *International Journal of Fatigue*, 164: 107128.
- [9] Yosri, A., Zayed, A., Saad-Eldeen, S., Leheta, H. (2021). [Influence of stress concentration on fatigue life of corroded specimens under uniaxial cyclic loading](#). *Alexandria Engineering Journal*, 60(6):5205–5216.
- [10] Jakubowski, M. (2015). [Influence of Pitting Corrosion on Fatigue and Corrosion Fatigue of Ship and Offshore Structures, Part II: Load - Pit - Crack Interaction](#). *Polish Maritime Research*, 22(3):57–66.
- [11] Liang, X., Sheng, J., Wang, K. (2019). [Investigation of the mechanical properties of steel plates with artificial pitting and the effects of mutual pitting on the stress concentration factor](#). *Results in Physics*, 14: 102520.
- [12] Mendes, P. J. S. C. (2018). *Stress Concentration Factor Evaluation in Offshore Tubular KT-Joints for Fatigue design*. Mestrado Integrado em Engenharia Civil - 2017/2018 - Departamento de Engenharia Civil, Faculdade de Engenharia da Universidade do Porto, Portugal.
- [13] Aidibi, A., Babamohammadi, S., Fatnuzzi, N., Correia, J. A. F. O., Manuel, L. (2021). [Stress Concentration Factor Evaluation of Offshore Tubular KT Joints Based on Analytical and Numerical Solutions: Comparative Study](#). *Practice Periodical on Structural Design and Construction*, 26(4).
- [14] Chinh, V. D., Nguyen, H. T. T. (2022). [Numerical models for stress analysis of non-uniform corroded tubular members under compression](#). *Structural Engineering and Mechanics*, 84(4):517.

- [15] Althaf, M., Navvar, K. M., Prakash, G., Varghese, N., Navaneeth, C. A. (2021). [Computation of stress concentration factor of tubular joints for the fatigue analysis of steel structures](#). *IOP Conference Series: Materials Science and Engineering*, 1114(1):012009.
- [16] Dassault Systèmes Simulia Corp (2011). *Abaqus/CAE User's Manual*. USA.
- [17] Kumar, L., Kumar, A., Barnat-Hunek, D., Szczygielska, E., Garbacz, M. (2019). [SCFs study of tubular T/Y steel joints under inplane loading](#). *MATEC Web of Conferences*, 252:06010.
- [18] Mohamed, H. S., Shao, Y., Chen, C., Shi, M. (2021). [Static strength of CFRP-strengthened tubular TT-joints containing initial local corrosion defect](#). *Ocean Engineering*, 236:109484.
- [19] Lesani, M., Hosseini, A. S., Bahaari, M. R. (2022). [Load bearing capacity of GFRP-strengthened tubular T-joints: Experimental and numerical study](#). *Structures*, 38:1151–1164.
- [20] ABS (2014). *Guidance for Fatigue Assessment of Offshore Structures*. American Bureau of Shipping.